ACS Sustainable Chemistry & Engineering

Research Article

pubs.acs.org/journal/ascecg

Encapsulation of a Biobased Lignin–Saponite Nanohybrid into Polystyrene Co-Butyl Acrylate (PSBA) Latex via Miniemulsion Polymerization

Suguna Jairam,[†] Zhaohui Tong,*[,†] Letian Wang,[†] and Bruce Welt[†]

[†]Department of Agricultural and Biological Engineering, University of Florida, P.O. Box 110570, Gainesville, Florida 32611, United States

ABSTRACT: In this study, lignin recovered from a biorefinery waste stream was used to modify a clay saponite to form a lignin–clay nanohybrid. Approximately 32 wt % of lignin was associated into a lignin–clay nanohybrid, which could be well dispersed into an organophilic monomer phase. This nanohybrid was then encapsulated into polystyrene co-butyl acrylate (PSBA) particles to form stable latex via in situ miniemulsion polymerization. The final latex had a broad size distribution and a narrow window of the nanohybrid (1.9–5.3 wt %) loading level. X-ray powder diffraction (XRD), transmission electron microscopy (TEM), and scanning electron microscopy (SEM) analysis of latex films indicated successful encapsulation of intercalated nanohybrids inside a copolymer matrix. The introduction of lignin–clay nanohybrids greatly improved PSBA properties. The nanocomposite with a 5.3% nanohybrid had a 13.75 times increase in tensile strength, an approximate 50 °C increase in degradation temperature, and a 42% decrease in oxygen permeability.

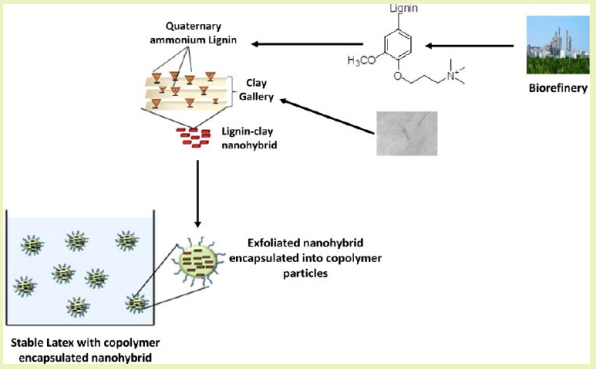

KEYWORDS: *Biobased, Lignin–clay nanohybrid, Miniemulsion polymerization, Encapsulation, Stable latex*

INTRODUCTION

Much effort has recently been directed to the study of increasing the renewable portion of petroleum-based products[1−3] including the use of environmentally friendly solvent and recycled materials. Meanwhile, biobased products still need to meet the ever-growing functional requirements such as having a better barrier for water, gas, and heat; improved mechanical properties; and biocompatibility.[4,5] The reorganization and self-assembling of multiphase materials in nanometer scale (e.g., nanoclay) into a polymer matrix has been considered as an effective approach to improve these functional properties.[6−8] Polymer nanoclay composites, which incorporate inorganic clay within a polymer matrix with at least one dimension in nanometer scale (10^{-9} m),[9] have gained great attention because of their excellent properties such as improved mechanical properties, low permeability to gas and heat, and chemical seal.[10−14] The improved properties of those composites are due to well-dispersed nanoscale inorganic layered materials into a polymer matrix.[15] If the polymer can thoroughly penetrate the clay platelet, the clay loses its crystallographic register to form an exfoliated clay platelet. The exfoliated clay–polymer composites exhibit desirable properties even in a considerably small loading,[16−18] which possess great potential as coating materials, especially in food packaging.[19−21]

Polymer nanocomposite in an aqueous phase has many advantages over its bulk[22−26] and solvent[27,28] forms in terms of safety, sustainability, and energy- and cost-effectiveness. However, emulsion can be easily broken up during handling or when mixed with foreign materials such as pigments and fillers. The stability of emulsion becomes a concern. Encapsulation is an effective approach to obtain stable latex through improving the interfacial bonding between a polymer matrix and nanophase. If the foreign particles (inorganic particles or their hybrids) can be well dispersed into polymer particles through encapsulation during the polymerization process, stable emulsion can be formed successfully.

Miniemulsion polymerization is an in situ polymerization technique that enables efficient encapsulation of inorganic phases within polymer droplets and ensures uniform nanophase dispersion and narrow particle size distribution.[29,30] These types of miniemulsions, as being recently discovered, include polymer-encapsulated oxides of titanium and iron,[31,32] adhesives,[33] drug release agents,[34,35] dyes, etc. The inorganic phases in these miniemulsions are spherical particles with narrow particle size distributions, which are conducive to better encapsulation into polymer droplets in solution. Clays, however, are composed of stacked platy lamellar structures and have broader particle size distributions, which impede the encapsulation into spherical polymer particles during the polymerization process. In addition, pristine clay is hydrophilic

Received: August 28, 2013
Revised: September 17, 2013
Published: September 22, 2013

and should be modified to organophilic in order to be compatible with the organophilic monomer or polymer.[36−38] Smectite clays have lamellar structures composed of hydrated cations located between the layers and the edges, which may facilitate the intercalation of cationic surfactants. However, previous research indicated that surfactant characteristics including chain length and functional groups have played important roles in surface properties, maximum loadings of nanophases, latex stability, and encapsulation efficiency.[38,14]

In this paper, we focus on the use of modified lignin recovered from a biorefinery waste stream as a biobased surfactant to penetrate into the clay plates for further encapsulation. Lignin, a highly cross-linked aromatic polymer of phenylpropane units, presents a significant portion (roughly 18−35%) of lignocellulosic biomass.[39] It is usually reclaimed from waste streams of the biorefining and papermaking processes. In this study, lignin was at first modified to a cationic form by the incorporation of quaternary ammonium groups, which could interact with the hydroxyl groups on the clay plates resulting in swelling, exfoliation, and further delamination. Then, stable latex of a polystyrene butyl acrylate (PSBA)-encapsulated lignin−clay nanohybrid was successfully synthesized via in situ miniemulsion polymerization. To the best of our knowledge, this is the first time to use lignin, a biobased waste, to modify a clay surface to form a lignin−clay nanohybrid, with further encapsulation of this nanohybrid within polymer droplets.

MATERIALS

The lignin was extracted from the fermentation broth of a bioethanol process, which involves liquefaction plus a simultaneous saccharification and fermentation process (L+SScF) using sugar cane bagasse as the raw materials.[40] Na-saponite clay was kindly provided by Kunimine Industries Co., Ltd. (Japan). It was synthesized by a hydrothermal reaction with an ideal formula of $(Na_{0.49}Mg_{0.14})^{0.77+}$ $[(Si_{7.20}Al_{l0.80})-(Mg_{5.97}Al_{0.03})\ O_{20}\ (OH)_4]^{0.77-}$. The cationic exchange capability (CEC) of Na-saponite is 0.712 equiv/kg. Trimethylamine (TMA, 50% aqueous solution), epichlorohydrin (ECH, 99%), styrene (99%), and butyl acrylate were purchased from Acros Organics (U.S.A.). Styrene was washed with 5 wt % NaOH followed by deionized water until pH 7 was reached and vacuum distilled at 74 °C before use. Butyl acrylate was vacuum distilled before use. Tetrahydrofuran (HPLC grade) was purchased from Fisher Scientific (U.S.A.), and 2, 2 azo-isobutyronitrile (AIBN), Triton 405 (TX-405, 4-(C_8H_{17})-$C_6H_4(OCH_2CH_2)_{40}OH$, 70% solution in water), and hexadecane (>99%) were purchased from Aldrich Chemical Inc. (U.S.A.) and used as purchased. Silver nitrate, 0.025 M, was purchased from Ricca Chemicals (U.S.A.).

METHODS

Alkaline Extraction of Lignin. The fermentation broth collected from a cellulosic bioethanol process was washed using the test sieve with U.S. standard #270 mesh size under warm water until the effluent became clear, and then it was dried in an oven at 70 °C for at least 24 h. To ensure the best lignin yield and purity, this residue was then treated in a blender for about 1 min and passed through two test sieves stacked in series with U.S. standard #20 mesh and #80 mesh, respectively. Residues left between the two sieves were collected. Lignin was extracted from the collected residues using a method modified from the method reported by Li et al.[41] At first, residues were subjected to an alkaline extraction by 2 M NaOH (residue/NaOH = 1:10 by weight) at 60 °C in an incubator/shaker at 150 rpm for 60 min. The black-brown supernatant was collected by centrifugation at 5000 rpm for 15 min. This supernatant was then neutralized by 5 M sulfuric acid until the pH reached 4. Brown precipitates were then isolated by filtration under vacuum and dried in vacuum at 40 °C to obtain alkaline extractable lignin. Lignin was analyzed by the National Renewable Energy Laboratory (NREL) procedure,[42] and the results showed that its purity was higher than 95%.

Surface Modification of Saponite Using Alkaline Extracted Lignin. *Synthesis of Epoxypropyl Trimethylammonium Chloride (ETAC).* The synthesis of ETAC from trimethylamine (TMA) and epichlorohydrin (ECH) is demonstrated in Scheme 1 (a). According to Wu et al.'s method,[43] the mixture of TMA and ECH with a molar ratio of 10:7 was transferred to a tri-neck flask installed with a condenser and a stirrer in an ice−salt bath (NaCl/ice = 1:3 by weight) for 1 h. After that, the reactants were left overnight for complete reaction. ETAC can be detected by silver nitrate with the appearance of white precipitate and is ready for preparation of quaternary ammonium lignin.

Scheme 1. Chemical reactions. (a) Synthesis of Epoxypropyl Trimethylammonium Chloride (ETAC). (b) Synthesis of Quaternary Ammonium Lignin (QAL)

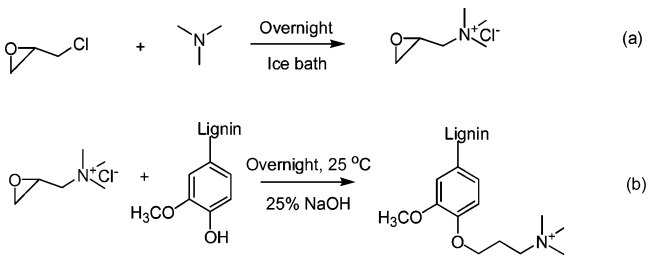

Synthesis of Quaternary Ammonium Lignin (QAL). At first, 2.5 g of lignin was reacted with 25 mL of a NaOH (20 wt %) solution in a warm bath at 80 °C for 20 min. Then, ETAC was added into the mixture, and the reaction was conducted under constant magnetic stirring for 5 h until a brown-red emulsion was obtained. The chemical reaction refers to Scheme 1(b). The obtained products were dried under vacuum and stored in a refrigerator prior to use.

Surface Modification of Saponite by QAL. A suspension of 5 g of saponite in 400 mL of deionized water was continuously stirred for 5 h until a transparent suspension was obtained. Then a suspension of 8−10 g of QAL dispersed in 100 mL of deionized water was added into the saponite suspension and stirred overnight. The gel-like yellowish product was isolated by centrifugation. After that, the product was repeatedly washed with ethanol and water and then separated by centrifugation at 15,000 rpm to remove excess ETAC and QAL until no chloride could be detected by silver nitrate. The formed lignin−clay nanohybrid was then dried in vacuum at room temperature.

Miniemulsion Polymerization of Styrene and Butyl Acrylate (BA) in the Presence of Lignin−Clay Nanohybrid. In a typical run, the oil phase composed of 1.2 g of co-stabilizer hexadecane, 0.24 g of AIBN, 7.2 g of monomer styrene, 4.8 g of monomer butyl acrylate, and varying quantities of lignin−clay nanohybrid was stirred at room temperature for 30 min followed by ultrasonication in an ice bath for 4 min. This mixture was poured into a water phase containing 1g of TX-405 in 100 g of water and then placed in an ice bath and magnetically stirred for 30 min. After that, the miniemulsion was formed by ultrasonication for another 3 min. The resulting miniemulsion was poured into a three-necked flask equipped with a condenser and a temperature sensor and magnetically stirred for another 30 min at room temperature by degassing with nitrogen. The polymerization was conducted by increasing the temperature to 80 ± 2 °C and keeping at that temperature for 6 h under continuous magnetic stirring. The reaction was terminated by adding a few drops of 2% 4-methoxy-phenol into the miniemulsion. The typical recipe is shown in Table 1. Films were casted by drying the emulsion in an oven on a flat plate at 60 °C for 12 h. The nanohybrid loading ratio was calculated by reduction of the rejected large nanohybrid aggregates during ultrasonication.

Characterization. Fourier transform infrared spectrometry (FTIR) spectra were recorded on a Magna System 560 from Nicolet

Table 1. Basic Recipe for Synthesis of Co-Butyl Acrylate Encapsulated Lignin−Clay Nanohybrid Latex via Miniemulsion Polymerization

mixtures	component	amount added (g)	percentage in total (wt %)	percentage in monomer (wt %)
oil phase A	styrene	7.2	6	60
	butyl acrylate	4.8	4	40
	hexadecane	1.2	1	10
	lignin−clay nanohybrid	0.228, 0.3, 0.636	0.19−0.53	1.9− 5.3
	AIBN	0.24	0.2	2
water phase B	TX-405	1	0.9	8.3
	DI water	100	87	833

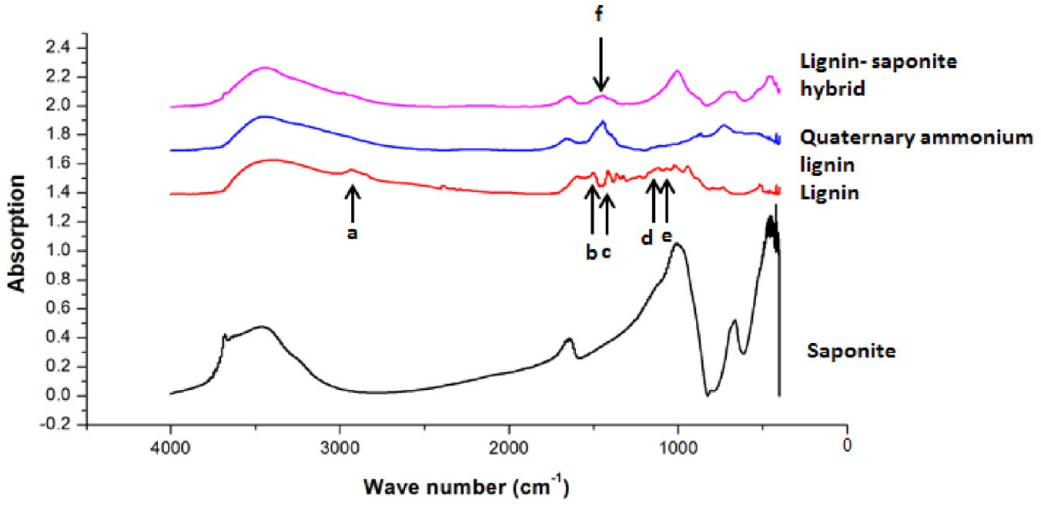

Figure 1. FTIR analysis of pristine saponite, lignin, quaternary ammonium lignin, and lignin−saponite nanohybrid with KBr Pellets. Characteristic stretching and vibration wave numbers are labeled (a = 3000 cm^{-1}, b = 1490 cm^{-1}, c = 1450 cm^{-1}, d = 1210 cm^{-1}, e = 1145 cm^{-1}, and f = 1429 cm^{-1}).

Instrument (WI, U.S.A.) using samples mixed with potassium bromide (KBr) (0.5% w/w to KBr) in pellet form. The molecular weight of lignin was measured by size exclusion chromatography (SEC), an Agilent Technologies 1260 series HPLC system equipped with a refractive index detector (RID), and a multiple wavelength detector (MWD) (CA, U.S.A.). Three columns were connected in series including PLgel-mixed B, PLgel-mixed E (5 μm with a pore size of 10,000 Å), and PLgel-mixed E (5 μm with a pore size of 100 Å). Lignin was acetylated according to the method described by Pan et al.[44]and then dissolved in HPLC-grade tetrahydrofuran for 8 h at a concentration of approximately 0.5 wt %. Then the solution was filtered through a 0.22 μm syringe filter before injections to remove undissolved materials such as cellulose and lignin. Twenty microliters of filtered solution was injected in each run at a thermostat temperature of 25 °C and a flow rate of 1 mL/min. All results were processed using the ChemStation software package with gas permeation chromatography (GPC) analysis (Rev.B.04.03). The molecular weight was calculated based on a universal calibration using a set of polystyrene standards.

Thermogravimetric analysis was performed using a Mettler Toledo (OH, U.S.A.) thermal analyzer at a heating rate of 20 °C/min and at a temperature up to 1000 °C. Dynamic light scattering (DLS) (Zetasizer ZS3600 with a noninvasive back scatter under 500 mw and a 532 nm laser, Malven, U.K.) was used to estimate the size and size distribution of the miniemulsion. Mechanical testing of composite films was performed on an Instron test machine (Model 5566, load cell capacity of 40 N, Instron instruments, Grove City, PA, U.S.A.) with a crosshead speed of 10 mm/min or 100 mm/min. The crosshead extension was used as specimen deformation. In accordance with ASTM standards D1708,[45] samples were cut to the dog-bone shape with a width of 5 mm, length of 24 mm for the narrow portion (gauge length 8 mm), and total length of 40 mm. Five replicates were tested for each composite. Tensile moduli of all composites were determined from the linear portion of the stress−strain curves (tangent modulus). Oxygen transmission rates (OTR) were measured using permeation cells and fluorescence oxygen detection equipment from Oxysense, Inc. (Model 301, TX, U.S.A.) by the dynamic accumulation (DA) method as described by Welt and Abdellatief.[46] Composite film with a uniform thickness of 0.05 mm and an area of 3.14 cm^2 was used to estimate OTR values. Films were sealed in an aluminum cast to avoid gas leaks and accidental film breakage.

Transmission electron microscopy (TEM) and scanning electron microscopy (SEM) were carried out to study the morphologies of latex particles and melting latex films. TEM was conducted on a JEOL 200CX instrument (JEOL instruments, MA, U.S.A.) with 100 keV accelerating voltage and using carbon type A grids. X-ray powder diffraction (XRD) patterns were recorded to measure *d*-spacing of clay galleries before and after intercalation using the Philips X'Pert MRD system. SEM was carried out on a FEI XL 40 FEG SEM (FEI instruments, OR, U.S.A.) at an operation voltage of 10 keV. Emulsion samples were dried on carbon tabs and coated with gold palladium coating (Au/Pd). XRD measurements were performed on Phillips XPert MRD instrument Cu K radiation source (λ = 1.54056 Å) at a generator voltage of 45 V, step size of 0.02°, and scan step time of 2 s. The d (001) basal-spacings of the original clay, modified lignin−clay nanohybrid, and its polymer composites were calculated using the Bragg equation: d = λ/2 sin θ.

RESUTS AND DISCUSSION

Cationic Modification of Lignin and the Formation of Lignin−Clay Nanohybrid. To facilitate encapsulation of nanophase within the polymer droplets, the nanohybrid was made hydrophobic and then well-dispersed into the monomer phase before miniemulsion polymerization.[36,47] The alkaline-extracted lignin had the weight average molecular weight (M_w)

of 3843.9, and its polydispersity index of M_w/M_n was 3.60. When dispersed in an oil−water system, this lignin behaved like a surfactant by staying between the water−oil phases. However, it was not capable of insertion into clay galleries without modification due to the lack of active groups that could react with the hydroxyl groups of clay. Therefore, in this study, we first modified lignin by ETAC to form cationic lignin through grafting quaternary ammonium groups as shown in Scheme 1. The produced cationic lignin could dissolve in water and subsequently associate with water-dispersed clay at its anionic sites. The produced lignin−clay nanohybrid was compatible with the organophilic co-monomer (styrene−butyl acrylate) phase. When this lignin-based nanohybrid was dispersed in the co-monomer via ultrasonication, we observed that miniemulsions were stable only in a very narrow window of lignin−clay nanohybrid concentrations from 1.6 to 5.2 wt %. It was also observed that the viscosity of the co-monomer phase was increased as the lignin−clay nanohybrid loading level increased. High molecular weight and network structure of lignin might cause the increased viscosity of the organophilic phase (nanohybrid in co-monomer) in comparison with other commercial surfactants with single carbon chains such as OTAB.[14] This agreed well with previous results for polystyrene-encapsulated nanoclay miniemulsions using cationic surfactants with different chain lengths.[21,38] As reported, high viscosity of the organophilic phase resulted in a decease in miniemulsion stability at high loading of nanohybrids. The stable miniemulsion was used for subsequent polymerization, and the composite latex obtained after polymerization was very stable for about 7 months when left to stand. Also, no remarkable precipitate was observed after centrifugation at 10,000 rpm for 10 min indicating high stability of the produced polymer latex.

TGA analysis was conducted to determine the weight percentage of cationic lignin absorbed with the clay. It was found that approximately 30.35 ± 0.15 wt % of lignin was absorbed with the clay together. We observed that the lignin−clay nanohybrid was located in the oil phase instead of the water phase in an oil−water system, which indicated the hydrophobicity of the produced lignin−clay nanohybrid. FTIR spectra of the lignin, quaternary ammonium lignin, saponite, and lignin−clay nanohybrid shown in Figure 1 indicate the entry of the lignin into the clay galleries.[48] Characteristic C−C stretching is seen at 3000 cm^{-1} (a) from the purified lignin and nanohybrid samples. Further, a phenolic ring vibration is seen at 1490 cm^{-1} (b), and group phenolic OH vibration is seen at 1450 and 1210 cm^{-1}(c, d, respectively), including an aryl−ether vibration observed at 1145 cm^{-1} (e) indicating the characteristic groups in the lignin molecular structure. Specifically, characteristic tertiary amine stretching at 1429 cm^{-1} (f) is observed in both modified lignin, with greatly reduced intensity in lignin−clay nanohybrid samples, and completely absent from the purified lignin sample. This provides evidence for the association between saponite and cationic lignin in molecular level.

X-ray diffraction (XRD) was used to detect the intercalation of clay in the pristine clay, lignin−clay nanohybrid, and polymer−nanohybrid composite as shown in Figure 2. Brad peaks were observed for all three samples. A distinct peak was not observed in pristine clay, and a similar observation was reported by Wang et al.[49] The pristine clay had a peak around the 2θ angle of 6.6° with an interlayer spacing of 1.34 nm. The interlayer spacing of the lignin−clay nanohybrid was increased to 1.52 nm at the peak around 5.8°. The peak of the polymer−nanohybrid composite disappeared, which indicated full exfoliation of the clay nanohybrid within the polymer matrix.

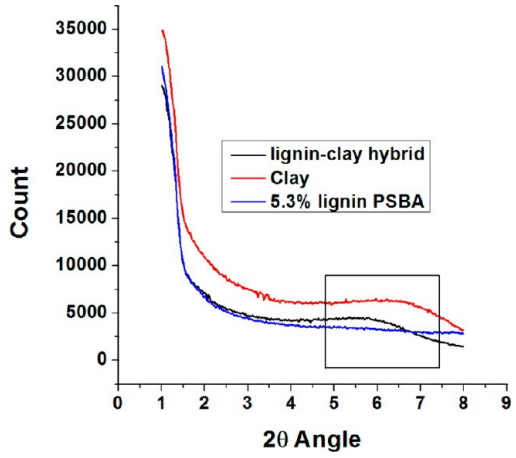

Figure 2. XRD spectra of pristine saponite, lignin−saponite nanohybrid, and polystyrene co-butyl acrylate (PSBA) composite latex.

Morphology and Particle Size of Final Composite Latex. TEM imaging of the polymer miniemulsion was conducted by placing a drop of emulsion on a grid and then drying at room temperature before observation. TEM and SEM images in Figure 3 clearly show the morphologies of latex particles, which include a majority of small spherical particles and a small number of large particles with spherical and hemispherical morphologies.

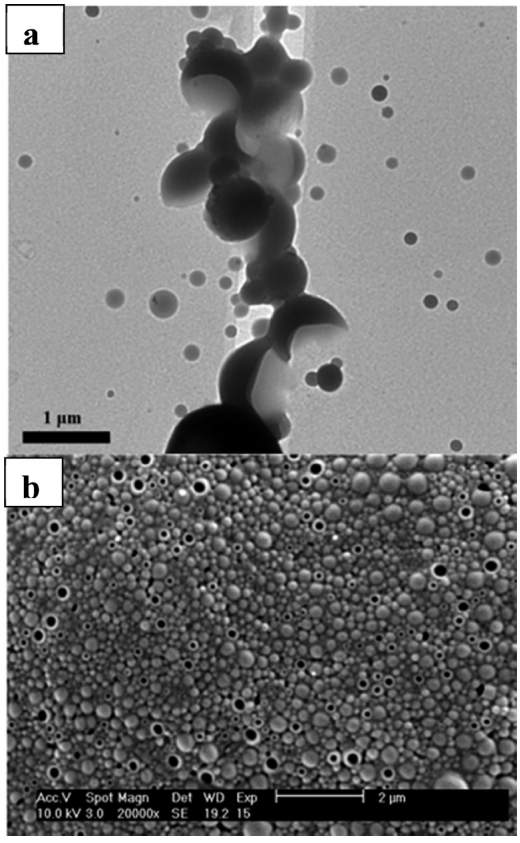

Figure 3. TEM (scale = 1 μm) (a) and SEM images (scale = 2 μm) (b) of the composite latex of polystyrene -co-butyl acrylate (PSBA)-encapsulated lignin−clay nanohybrid.

dx.doi.org/10.1021/sc4003196 | ACS Sustainable Chem. Eng. 2013, 1, 1630−1637

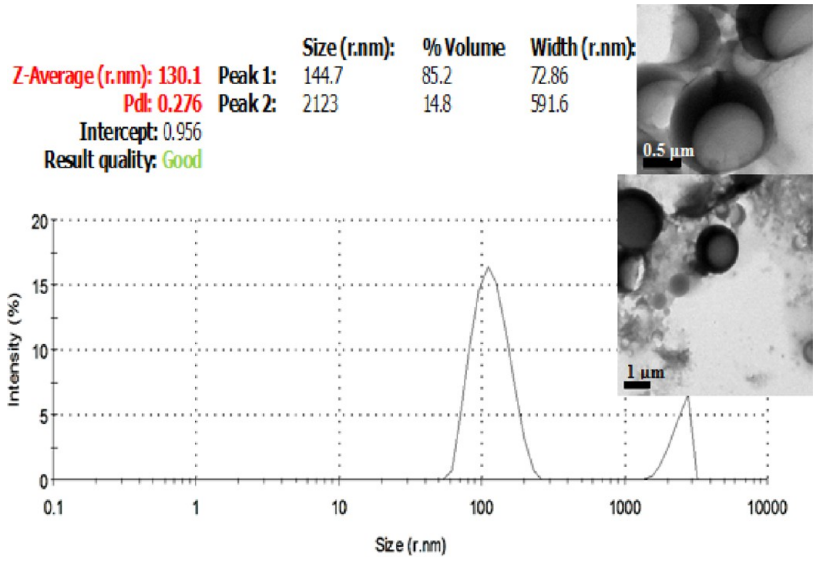

Figure 4. Particle size distribution and TEM images of composite latex of PSBA-encapsulated lignin−clay nanohybrid.

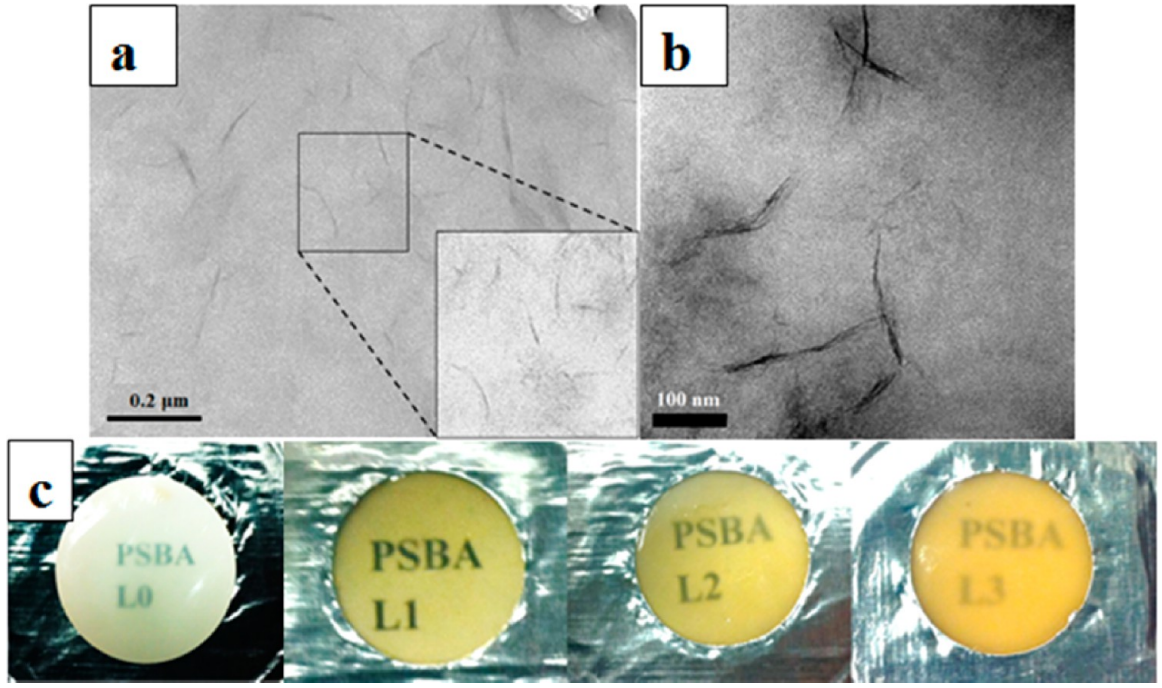

Figure 5. TEM images of (a) stable composite latex film of polystyrene co-butyl acrylate (PSBA)-encapsulated lignin−clay nanohybrid after melting and (b) unstable latex film of polystyrene co-butyl acrylate (PSBA) with unmodified saponite. (c) Film images showing lack of micro-aggregates for each lignin−clay loading level (L0 = 0% lignin (PSBA control), L1 = 1.9% lignin−clay loading, L2 = 2.5% lignin−clay loading, and L3 = 5.3% lignin loading).

In order to further clarify the particle size and its distribution, latex was further diluted, and its particle size was measured by dynamic light scattering (DLS) as shown in Figure 4. Two peaks were observed. One large peak with an average particle size of 144.7 nm in radius indicated dominant small particles in the latex. Another small peak with an average particle size of micrometers was attributed to the small number of large particles.

The DLS result was in agreement with the associated TEM images shown in Figures 3 and 4. Also, there was no indication of clay particles (irregular belt-like shape) attached on the surface of polymer particles and throughout the grid, which indicated that nanohybrid was successfully encapsulated into the co-polymer particles.

In order to clarify the intercalation of nanohybrids inside the polymer matrix, latex samples on the TEM grids were heated to a temperature higher than the co-polymer PSBA melting temperature to allow the dispersion of the co-polymer matrix into thin films. Figure 5 shows the TEM images of melted composite films in the presence of a lignin−clay nanohybrid, unmodified clay, and macroscopical composite film images with different loading levels of nanohybrids. When using unmodified saponite, unstable latex was formed after miniemulsion polymerization under the same reaction conditions. The

dx.doi.org/10.1021/sc4003196 | ACS Sustainable Chem. Eng. 2013, 1, 1630−1637

stacked clay layers were clearly shown in the images of melting composite films with unmodified saponite (Figure 5b). Different from the films with unmodified clay, the composite films with encapsulated lignin−clay nanohybrids had smooth surfaces with delaminated clay galleries (Figure 5a). This result provides evidence that in stable latex exfoliated nanohybrids were successfully distributed inside the co-polymer matrix. Further, Figure 5(c) indicates the absence of nanoaggregates of lignin-based nanohybrids in the synthesized films. Films produced were smooth, uniform, and transparent with a yellowish tint.

Thermal Stability of Composites. Thermogravimetric analysis (TGA) was used to evaluate the thermal stability of PSBA and its composite films in the addition of lignin−clay nanohybrids. As shown in Figure 6, PSBA nanohybrid

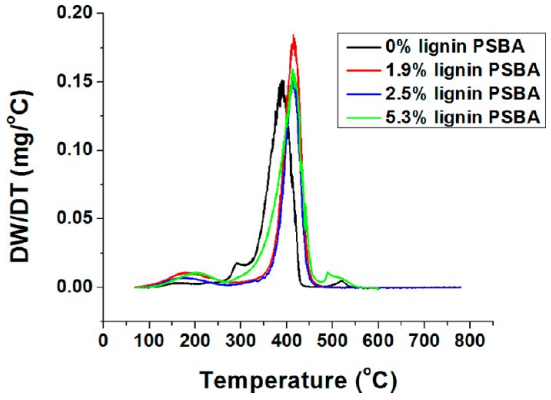

Figure 6. Thermogravimetric analysis (TGA) of pure polystyrene co-butyl acrylate (PSBA) latex film and the composite films with different loading levels of lignin−clay nanohybrids.

composite films degraded at a higher temperature than the pure co-polymer films. However, The loading ratios from 1.9% to 5.3% had no effect on the degradation temperature of the composites. The higher degradation temperature of all the composites indicated that the degradation of the clay and lignin in the nanophase of the composites occurred at a higher temperature than its polymer matrix. Similar studies including the encapsulation of nanoclay like cloisite and montmorillonite[10,50,51] have reported some improvement in thermal and mechanical properties, but the margin of improvement seen in the present study (approximately a 50 °C increase) is significant. Lignin may also contribute to the increase in degradation temperature because it has a broad range of degradation temperature from 200 to 500 °C,[52] which is higher than that of the co-polymer as well.

Tensile Strength of Composites. Tensile strengths (maximal stress) and the Young's moduli of pure PSBA latex film and composite films (styrene:butyl acrylate = 60:40) in the presence of 1.9−5.3 wt % of lignin−clay nanohybrids are illustrated in Figure 7. During the measurement, the pure co-polymer film showed high elastic property (low Young's modulus) by observing the film stretching to the machine's limit at a strain rate of 10 mm/min and was not able to be broken at that rate. Hence, the strain rate of the pure polymer film was adjusted to 100 mm/min compared to 10 mm/min for all the composites films. This phenomenon provided intuitionistic evidence that nanohybrids increased the Young's modulus (stiffness) of the PSBA films. Regarding all the nanocomposites, both Young's modulus and tensile strengths of

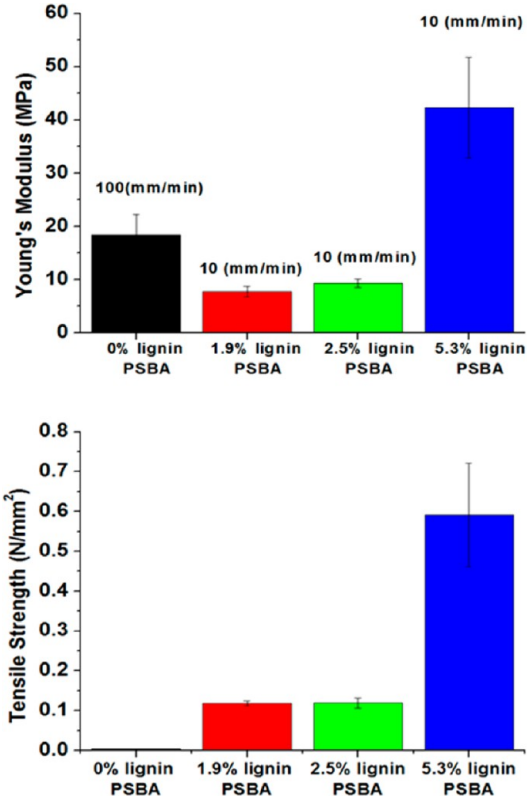

Figure 7. Young's moduli (top) and tensile strengths (bottom) of pure polystyrene co-butyl acrylate (PSBA) latex film at a 100 mm/min strain rate and composite films with different loading levels of lignin−clay nanohybrids at 10 mm/min strain rate.

the composite films were greatly improved with an increase in nanohybrid loading. This can be explained by exfoliated clays providing tremendous surface areas to aid the stress transfer of the reinforced composites. Even in the presence of 1.9 wt % of lignin−clay nanohybrids, a significant increase in tensile strength from 0.004 N/mm^2 (pure co-polymer film) to 0.59 N/mm^2 (P value = 0.0001; α = 0.05; composite film) was noted. It can be concluded that the addition of the lignin-based nanohybrid components to the polymer matrix greatly increased the Young's moduli and maximum stresses of the composite films. The values reported are in tandem with reports from other work using a polystyrene co-butyl acrylate matrix.[52]

Oxygen Transmission Rates of Polymer Films. The gas barrier properties of the latex films were evaluated using the oxygen transmission rate (OTR) measured by the dynamic accumulation method. As shown in Figure 8, the oxygen transmission rate was decreased with increased loadings of lignin−clay nanohybrids. The OTR value (1338.19 mL/m^2/day) of the composite film with maximum loading of nanohybrids was significantly lower than that of pure PSBA film (2311.68 mL/m^2/day) (P value = 0.005; α = 0.05). This is because the exfoliation and good dispersion of nanohybrid plates increase the torturous path of gas diffusion through the film.

CONCLUSIONS

Lignin recovered from the biorefinery waste stream was used to synthesize s lignin−clay nanohybrid that could be successfully encapsulated into a polystyrene butyl acrylate (PSBA) co-

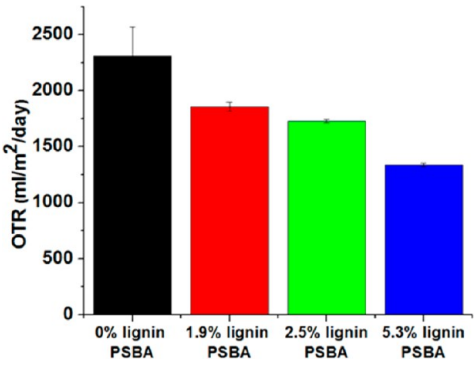

Figure 8. Oxygen transmission rates of pure polystyrene co-butyl acrylate (PSBA) latex film and composite films with different loadings of lignin–clay nanohybrids at 25 °C and 1 atm pressure.

polymer shell to form a stable composite latex via one-step miniemulsion polymerization. Lignin was at first modified to cationic lignin by ETAC, which entered clay galleries and enabled swelling and intercalation of clay galleries. Approximately 30 wt % of lignin was assembled with the saponite to produce an organophilic lignin–clay nanohybrid. It was known that premodification of the clay played an important role in the exfoliation of clay plates and hence stability of the latex. In this study, we found that an exfoliated lignin–clay nanohybrid could be encapsulated into the PSBA droplets to produce stable latex via miniemulsion polymerization. However, maximum lignin–clay nanohybrid loading could not be beyond 5.3 wt % due to the high viscosity of organophase, which may result from the high molecular weight of lignin. The introduction of a well-dispersed lignin–clay nanohybrid resulted in a notable increase in mechanical strength, gas barrier properties, and thermal stability of composite films in comparison with pure PSBA film. Our future research will seek to replace petroleum-based monomers by biobased monomers and evaluate how these sustainable elements (lignin–clay nanohybrid and biobased polymers) affect the functional properties of composite films and miniemulsion kinetics.

AUTHOR INFORMATION

Corresponding Author

*Telephone: 01-352-3921864. Fax: 01-352-3924902. Email address: ztong@ufl.edu.

Author Contributions

The manuscript was written through contributions of all authors. All authors have given approval to the final version of the manuscript.

Funding

This project has been co-supported by the Biomass Research & Development Initiative Competitive Grant 2001-10006-3058 from the U.S. Department of Agriculture and a United States–India Consortium Grant from the U.S. Department of Energy.

Notes

The authors declare no competing financial interest.

ACKNOWLEDGMENTS

The authors thank Dr. A. Brennan, Department of Material Science & Engineering, University of Florida, and Dr. L. Dempere, Major Analytical Instrumentation Center at University of Florida. We appreciate that the UF bioethanol pilot plant led by Dr. L. O. Ingram kindly provided the fermentation residues.

REFERENCES

(1) Ragauskas, A. J.; Williams, C. K.; Davison, B. H.; Britovsek, G.; Cairney, J.; Eckert, C. A.; Frederick, W. J., Jr; Hallett, J. P.; Leak, D. J.; Liotta, C. L.; Mielenz, J. R.; Murphy, R.; Templer, R.; Tschaplinski, T. The path forward for biofuels and biomaterials. *Science* **2006**, *311* (5760), 484–489.

(2) Dincer, I. Renewable energy and sustainable development: A crucial review. *Renewable Sustainable Energy Rev.* **2000**, *4* (2), 157–175.

(3) Ridley, C. E.; Clark, C. M.; Leduc, S. D.; Bierwagen, B. G.; Lin, B. B.; Mehl, A.; Tobias, D. A. Biofuels: Network analysis of the literature reveals key environmental and economic unknowns. *Environ. Sci. Technol.* **2012**, *46* (3), 1309–1315.

(4) Imran, M.; Revol-Junelles, A. M.; Martyn, A.; Tehrany, E. A.; Jacquot, M.; Linder, M.; Desobry, S. Active Food Packaging Evolution: Transformation from Micro- to Nanotechnology. *Crit. Rev. Food Sci. Nutr.* **2010**, *50* (9), 799–821.

(5) Mensitieri, G.; Di Maio, E.; Buonocore, G. G.; Nedi, I.; Oliviero, M.; Sansone, L.; Iannace, S. Processing and shelf life issues of selected food packaging materials and structures from renewable resources. *Trends Food Sci. Technol.* **2011**, *22* (2–3), 72–80.

(6) Carne, A.; Carbonell, C.; Imaz, I.; Maspoch, D. Nanoscale metal-organic materials. *Chem. Soc. Rev.* **2011**, *40* (1), 291–305.

(7) Dvir, T.; Timko, B. P.; Kohane, D. S.; Langer, R. Nanotechnological strategies for engineering complex tissues. *Nat. Nanotechnol.* **2011**, *6* (1), 13–22.

(8) Silvestre, C.; Duraccio, D.; Cimmino, S. Food packaging based on polymer nanomaterials. *Prog. Polym. Sci.* **2011**, *36*, 1766–1782.

(9) Rao, J. P.; Geckeler, K. E. Polymer nanoparticles: Preparation techniques and size-control parameters. *Prog. Polym. Sci.* **2011**, *36* (7), 887–913.

(10) Dash, S.; Kisku, S. K.; Swain, S. K. Effect of nanoclay on morphological, thermal, and barrier properties of albumin bovine. *Polym. Compos.* **2012**, *33* (12), 2201–2206.

(11) Herrera-Alonso, J. M.; Sedlakova, Z.; Marand, E. Gas transport properties of polyacrylate/clay nanocomposites prepared via emulsion polymerization. *J. Membr. Sci.* **2010**, *363* (1–2), 48–56.

(12) Diaconu, G.; Paulis, M.; Leiza, J. R. Towards the synthesis of high solids content waterborne poly(methyl methacrylate-co-butyl acrylate)/montmorillonite nanocomposites. *Polymer* **2008**, *49* (10), 2444–2454.

(13) Diaconu, G.; Paulis, M.; Leiza, J. R. High solids content waterborne acrylic/montmorillonite it nanocomposites by miniemulsion polymerization. *Macromol. React. Eng.* **2008**, *2* (1), 80–89.

(14) Tong, Z. H.; Deng, Y. L. Synthesis of water-based polystyrene-nanoclay composite suspension via miniemulsion polymerization. *Ind. Eng. Chem. Res.* **2006**, *45* (8), 2641–2645.

(15) Theng, B. K. G. *Formation and Properties of Clay–Polymer Complexes*; Elsevier Science Limited: Oxford, 2012; Vol. *4*, p 210.

(16) Panwar, A.; Choudhary, V.; Sharma, D. K. A review: Polystyrene/clay nanocomposites. *J Reinf. Plast. Comp.* **2011**, *30* (5), 446–459.

(17) Robello, D. R.; Yamaguchi, N.; Blanton, T.; Barnes, C. Spontaneous formation of an exfoliated polystyrene–clay nanocomposite using a star-shaped polymer. *J. Am. Chem. Soc.* **2004**, *126* (26), 8118–8119.

(18) Carrado, K. A. Synthetic organo- and polymer-clays: Preparation, characterization, and materials applications. *Appl. Clay Sci.* **2000**, *17* (1–2), 1–23.

(19) Mirzataheri, M.; Atai, M.; Mahdavian, A. R. Physical and mechanical properties of nanocomposite barrier film containing encapsulated nanoclay. *J. Appl. Polym. Sci.* **2010**, *118* (6), 3284–3291.

(20) Ku, B. C.; Froio, D.; Steeves, D.; Kim, D. W.; Ahn, H.; Ratto, J. A.; Blumstein, A.; Kumar, J.; Samuelson, L. A. Cross-linked multilayer polymer-clay nanocomposites and permeability properties. *J. Macromol. Sci. Pure* **2004**, *A41* (12), 1401–1410.

(21) Sun, Q. H.; Schork, F. J.; Deng, Y. L. Water-based polymer/clay nanocomposite suspension for improving water and moisture barrier in coating. *Compos. Sci. Technol.* **2007**, *67* (9), 1823−1829.
(22) Arora, A.; Choudhary, V.; Sharma, D. K. Effect of clay content and clay/surfactant on the mechanical, thermal and barrier properties of polystyrene/organoclay nanocomposites. *J. Polym. Res.* **2011**, *18* (4), 843−857.
(23) Frankowski, D. J.; Capracotta, M. D.; Martin, J. D.; Khan, S. A.; Spontak, R. J. Stability of organically modified montmorillonites and their polystyrene nanocomposites after prolonged thermal treatment. *Chem. Mater.* **2007**, *19* (11), 2757−2767.
(24) Su, S. P.; Jiang, D. D.; Wilkie, C. A. Study on the thermal stability of polystyryl surfactants and their modified clay nanocomposites. *Polym. Degrad. Stab.* **2004**, *84* (2), 269−277.
(25) Su, S. P.; Jiang, D. D.; Wilkie, C. A. Polybutadiene-modified clay and its nanocomposites. *Polym. Degrad. Stab.* **2004**, *84* (2), 279−288.
(26) Costache, M. C.; Heidecker, M. J.; Manias, E.; Gupta, R. K.; Wilkie, C. A. Benzimidazolium surfactants for modification of clays for use with styrenic polymers. *Polym. Degrad. Stab.* **2007**, *92* (10), 1753−1762.
(27) Morgan, A. B.; Harris, J. D. Exfoliated poly styrene-clay nanocomposites synthesized by solvent blending with sonication. *Polymer* **2004**, *45* (26), 8695−8703.
(28) Giannakas, A.; Spanos, C. G.; Kourkoumelis, N.; Vaimakis, T.; Ladavos, A. Preparation, characterization and water barrier properties of PS/organo-montmorillonite nanocomposites. *Eur. Polym. J.* **2008**, *44* (12), 3915−3921.
(29) Asua, J. M. Miniemulsion polymerization. *Prog. Polym. Sci.* **2002**, *27* (7), 1283−1346.
(30) Schork, F. J.; Luo, Y. W.; Smulders, W.; Russum, J. P.; Butte, A.; Fontenot, K. Miniemulsion polymerization. *Adv. Polym. Sci.* **2005**, *175*, 129−255.
(31) Madani, M.; Sanjani, N. S.; Majidi, R. F. Magnetic polystyrene nanocapsules with core−shell morphology obtained by emulsifier-free miniemulsion polymerization. *Polym. Sci., Ser. A* **2011**, *53* (2), 143−148.
(32) Muñoz-Espí, R.; Dolcet, P.; Rossow, T.; Wagner, M.; Landfester, K.; Crespy, D. Tin(IV) oxide coatings from hybrid organotin/polymer nanoparticles. *ACS Appl. Mater. Interfaces.* **2011**, *3* (11), 4292−4298.
(33) Bunker, S.; Staller, C.; Willenbacher, N.; Wool, R. Miniemulsion polymerization of acrylated methyl oleate for pressure sensitive adhesives. *Int . J . Adhes. Adhes.* **2003**, *23* (1), 29−38.
(34) Weiss, C. K.; Landfester, K. Miniemulsion polymerization as a means to encapsulate organic and inorganic materials. *Hybrid Latex Particles: Prep. with (Mini) Emulsion Polym.* **2010**, *233*, 185−236.
(35) Mamaghani, M. Y.; Pishvaei, M.; Kaffashi, B. Synthesis of latex based antibacterial acrylate polymer/nanosilver via in situ mini-emulsion polymerization. *Macromol. Res.* **2011**, *19* (3), 243−249.
(36) Zhou, C. H.; Shen, Z. F.; Liu, L. H.; Liu, S. M. Preparation and functionality of clay-containing films. *J. Mater. Chem.* **2011**, *21* (39), 15132−15153.
(37) Faucheu, J.; Gauthier, C.; Chazeau, L.; Cavaille, J. Y.; Mellon, V.; Bourgeat-Lami, E. Miniemulsion polymerization for synthesis of structured clay/polymer nanocomposites: Short review and recent advances. *Polymer* **2010**, *51* (1), 6−17.
(38) Tong, Z. H.; Deng, Y. L. Synthesis of polystyrene encapsulated nanosaponite composite latex via miniemulsion polymerization. *Polymer* **2007**, *48* (15), 4337−4343.
(39) Rogers, M. R. *Handbook of Wood Chemistry and Wood Composite*; Taylor & Francis Group: Boca Raton, FL, 2005; p 44.
(40) Geddes, C. C.; Mullinnix, M. T.; Nieves, I. U.; Peterson, J. J.; Hoffman, R. W.; York, S. W.; Yomano, L. P.; Miller, E. N.; Shanmugam, K. T.; Ingram, L. O. Simplified process for ethanol production from sugarcane bagasse using hydrolysate-resistant Escherichia coli strain MM160. *Bioresour. Technol.* **2011**, *102* (3), 2702−2711.
(41) Li, J. B.; Gellerstedt, G.; Toven, K. Steam explosion lignins; their extraction, structure and potential as feedstock for biodiesel and chemicals. *Bioresource Technol .* **2009**, *100* (9), 2556−2561.
(42) A. Sluiter, B. H., Ruiz, R.; Scarata, C.; Sluiter, J.; Templeton, D.; Crocker, D. *Determination of Structural Carbohydrates and Lignin in Biomass*; National Renewable Energy Laboratory (NREL): Golden, CO, 2011.
(43) Jiang, T., *Lignin*, 1st ed.; Chemical Industry Press: Beijing, China, 2001; p 195.
(44) Pan, X. J.; Kadla, J. F.; Ehara, K.; Gilkes, N.; Saddler, J. N. Organosolv ethanol lignin from hybrid poplar as a radical scavenger: Relationship between lignin structure, extraction conditions, and antioxidant activity. *J. Agric. Food Chem.* **2006**, *54* (16), 5806−5813.
(45) ASTM. D1708-10. *Standard Test Method for Tensile Properties of Plastics by Use of Micotensile Specimens*; ASTM: West Conshohocken, PA, 2010.
(46) Abdellatief, A.; Welt, B. A. Comparison of new dynamic accumulation method for measuring oxygen transmission rate of packaging against the steady-state method described by ASTM D3985. *Packag. Technol. Sci.* **2012**, DOI: 10.1002/pts.1974.
(47) Sun, Q. H.; Deng, Y. L.; Wang, Z. L. Synthesis and characterization of polystyrene-encapsulated laponite composites via miniemulsion polymerization. *Macromol. Mater. Eng.* **2004**, *289* (3), 288−295.
(48) Silverstein, R. M.; Webster, F. X. ; Kimle, D. *Spectrometric Identification of Organic Compounds*; John Wiley & Sons, Inc.: Hoboken, NJ, 2007; p 502.
(49) Wang, J. Z.; Wheeler, P. A.; Jarrett, W. L.; Mathias, L. J. Synthesis and characterization of dual-functionalized laponite clay for acrylic nanocomposites. *J. Appl. Polym. Sci.* **2007**, *106* (3), 1496−1506.
(50) Samakande, A.; Sanderson, R. D.; Hartmann, P. C. Encapsulated clay particles in polystyrene by RAFT mediated miniemulsion polymerization. *J. Polym. Sci. Pol . Chem.* **2008**, *46* (21), 7114−7126.
(51) LeBaron, P. C.; Wang, Z.; Pinnavaia, T. J. Polymer-layered silicate nanocomposites: An overview. *Appl .Clay Sci.* **1999**, *15* (1−2), 11−29.
(52) Manfredi, L. B.; Rodríguez, E. S.; Wladyka-Przybylak, M.; Vázquez, A. Thermal degradation and fire resistance of unsaturated polyester, modified acrylic resins and their composites with natural fibres. *Polym. Degrad. Stab.* **2006**, *91* (2), 255−261.